SPECIAL ISSUE

Nanogold-Enriched Carbon Nanohorn Label for Sensitive Electrochemical Detection of Biomarker on a Disposable Immunosensor

Changrong Zhao,[a, b] *Dajie Lin*,[a] *Jie Wu*,[a] *Lin Ding*,[a] *Huangxian Ju*,*[a] *Feng Yan**[c]

[a] State Key Laboratory of Analytical Chemistry for Life Science, Department of Chemistry, Nanjing University, Nanjing 210093, P. R. China
[b] School of Environmental Science and Public Health, Wenzhou Medical College, Wenzhou 325035, P. R. China
[c] Jiangsu Institute of Cancer Prevention and Cure, Nanjing 210009, P. R. China
*e-mail: hxju@nju.edu.cn; yanfeng2007@sohu.com

Received: August 3, 2012
Accepted: October 24, 2012
Published online: December 7, 2012

Abstract
A novel nanogold-enriched carbon nanohorn structure (nanoAu/CNH) was designed as a trace tag for highly efficient electrochemical detection of tumor marker using a disposable immunosensor. The nanoAu/CNH was synthesized by one-pot in situ growth of nanogold on carboxylated single-walled CNH. The labeling of signal antibody was performed via the inherent interaction between protein and nanogold. The disposable immunosensor was constructed by covalently cross-linking capture antibody on chitosan modified screen-printed carbon electrode. With a sandwich format, the nanoAu/CNH labeled antibody was conjugated on the immunosensor for electrochemical measurement of tumor marker by electrooxidizing the nanoAu at +1.3 V and then cathodic potential scan in 0.1 M HCl. Using α-fetoprotein as model target, the proposed immunoassay showed acceptable precision and wide linear range from 0.1 pg mL^{-1} to 1 ng mL^{-1} with a detection limit of 0.07 pg mL^{-1}. The new nanoAu/CNH label as well as the disposable immunosensor showed possessed potential application in point-of-care testing.

Keywords: Electrochemical immunoassay, Signal amplification, Single-walled carbon nanohorn, Nanogold, Screen-printed electrode

DOI: 10.1002/elan.201200423

1 Introduction

The early clinical diagnosis of cancer can greatly increase the success rate of disease treatment. As the levels of the tumor biomarkers in serum are associated with the stages of tumors, they can be used for screening and clinical diagnosis of cancer. The concentrations of most biomarkers are extremely low during the early stage of diseases, thus it is urgent to develop sensitive methods for the detection of low abundant proteins [1,2]. By combining with different signal amplification strategies, electrochemical immunoassay has become one of the most useful technologies for ultrasensitive detection of tumor markers due to its intrinsic advantages of good portability, low cost, easy operation, and high detection sensitivity [3–5]. The signal amplification can be achieved by simply loading a large amount of enzymes, electroactive molecules, or other signal elements on nanocarriers to label immunoreagents [6–13]. These nano-carriers include gold nanoparticles (AuNPs) [6–8], carbon nanomaterials [9–11], silica nanoparticles [12], and magnetic beads [13]. For example, horseradish peroxidase (HRP) has been loaded on AuNPs and carbon nanotubes to construct sensitive immunoassay methods for detection of human IgG [7] and cancer biomarkers [9,10].

The stripping analysis of AuNPs [14–16], silver nanoparticles [17,18] and quantum dots [19,20] has also shown great promise in sensitive immunoassay because one nanoparticle can release thousands of ions. These nanoparticles possess some advantages such as rapid and simple synthesis, narrow size distribution, convenient labeling to biomolecules, and good stability. AuNPs can be electrochemically oxidized in HCl to produce electroactive $AuCl_4^-$, which can then be reduced by a cathodic potential scan to produce detectable signal. In order to enhance the detection sensitivity, AuNPs have been assembled on another nano-carrier to label the signal antibody [21]. Here, a novel signal tag was designed by one-pot in situ growth of nanogold on dahlia flowerlike single-walled carbon nanohorns (SWCNHs). The formed nanogold-enriched carbon nanohorn structure (nanoAu/CNH) could conveniently be used as a label for electrochemical immunoassay.

SWCNHs, composed of thousands of graphitic tubule closed ends [22,23], are featured with large surface area, excellent conductivity, plentiful inner nanospaces, and

highly defective horns [24,25]. By oxidation treatment, extensive carboxyl sites can be produced on the cone-shaped tips to absorb poly(diallyldimethylammonium chloride) (PDDA). After functionalization with PDDA, $AuCl_4^-$ could easily adsorb on the surface of SWCNHs for chemical reduction to produce nanogold. More importantly, this structure was beneficial to the adsorption of the electrooxidation product, which could greatly improve the stability and detection precision. Using α-fetoprotein (AFP) as a model target, this work prepared a disposable immunosensor for sandwich-type immunoassay. This proposed method showed a detection limit down to 0.07 $pg\,mL^{-1}$, indicating a greatly improved sensitivity due to the high loading of nanogold. Owing to the advantages of easy design, simple operation, low cost and high sensitivity, this method provided potential application in clinical diagnosis.

2 Experimental

2.1 Materials and Reagents

SWCNHs were kindly provided by Professor Iijima (Japan Science and Technology Agency). Both mouse monoclonal capture antibody (Ab_1, clone No. bsm-1621) and signal antibody (Ab_2, clone No. bsm-1622) of AFP were purchased from Beijing Biosynthesis Biotechnology Co. Ltd. (Beijing, China). AFP standard solutions were gained from commercial AFP kit, which was supplied by Fujirebio Diagnostics AB (Göteborg, Sweden). Bovine serum albumin (BSA), PDDA (20%, w/w in water, MW: 200000–350000) and chitosan (CS, ≥85% deacetylation) were purchased from Sigma-Aldrich Chemical Co. (St. Louis, MO). Glutaraldehyde (GA, 25% aqueous solution) was purchased from Alfa Aesar China Ltd. Chloroauric acid ($HAuCl_4{\cdot}4H_2O$) and trisodium citrate were obtained from Shanghai Reagent Company (Shanghai, China). Sodium borohydride ($NaBH_4$) was obtained from Sinopharm Chemical Reagent Co., Ltd. (China). Phosphate buffered saline (PBS, 0.01 M, pH 7.4) containing 0.05% (w/v) Tween-20 and 5% (w/v) BSA were used as washing buffer and blocking buffer, respectively. Ultrapure water obtained from a Millipore water purification system (≥18 MΩ, Milli-Q, Millipore) was used in the whole assay. Clinical serum samples were from Jiangsu Institute of Cancer Research. All other reagents were of analytical grade and used as received.

2.2 Apparatus

The transmission electron micrographs (TEM) were gained on a JEM-2100 TEM (JEOL, Japan). X-ray photoelectron spectroscopic (XPS) measurements were performed with an ESCALAB 250 spectrometer (Thermo-VG Scientific, USA) with an ultrahigh vacuum generator. Scanning electron micrographs (SEM) were obtained with a Hitachi S-4800 scanning electron microscope (Japan) at an acceleration voltage of 10 kV. Differential pulse voltammetric (DPV) measurements were performed on a CHI 630D electrochemical workstation (Shanghai CH Instruments Co., China).

2.3 Synthesis and Bioconjugation of nanoAu/CNH

As shown in Scheme 1A, SWCNHs were firstly dispersed in 30% HNO_3 and then refluxed for 24 h at 140 °C to

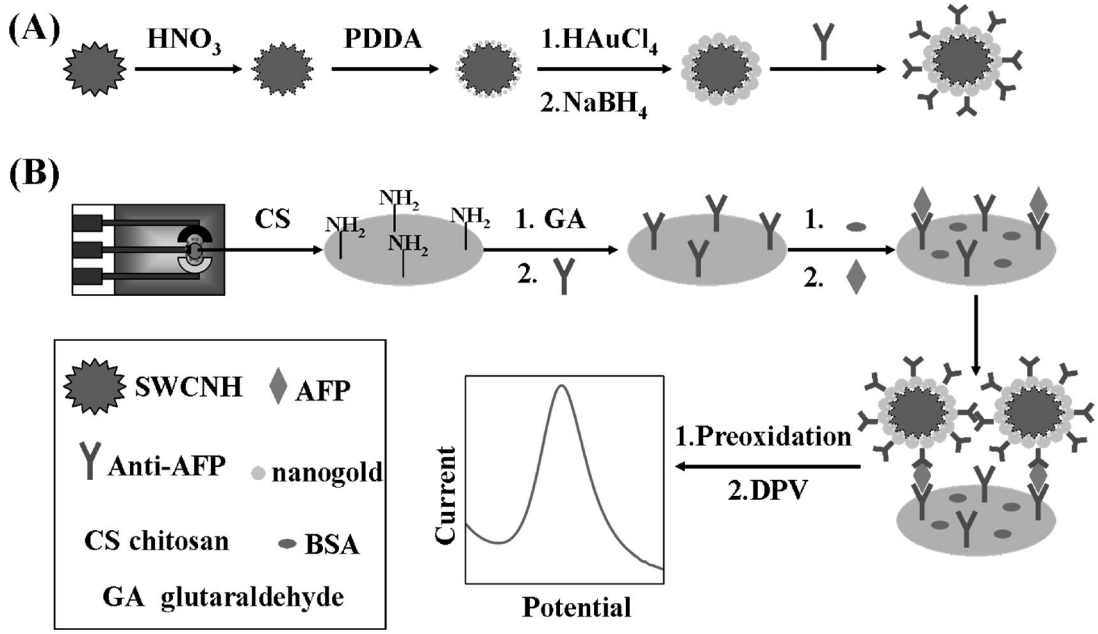

Scheme 1. Schematic representation of (A) Ab_2/nanoAu/CNH preparation and (B) immunosensor fabrication for sandwich-type immunoassay.

obtain carboxylic group-abundant SWCNHs. After centrifugation, the sediment was washed with water until the pH reached 7.0 and then dispersed in ultrapure water to obtain the concentration of 1 mg mL^{-1}. 1 mL of the above carboxylated SWCNHs was added into 1 mL of 0.20% PDDA aqueous solution containing 0.5 M NaCl and stirred for 40 min to assemble the PDDA layer on SWCNHs. Residual PDDA was removed by centrifugation (12000 rpm), and the precipitate was redispersed in 8 mL water. Then, 20 μL of both $HAuCl_4$ (25 mM) and 1% trisodium citrate were added to the solution of polyelectrolyte functionalized SWCNH under vigorous stirring in an ice-water bath for 30 min, followed by addition of 50 μL of freshly prepared ice-cold $NaBH_4$ (0.1 M) and vigorous stirring for 2 min. The resulting nanoAu/CNH was collected by centrifugation (5500 rpm) and washing with water, and dispersed in 4 mL of 10 mM pH 9.0 Tris-HCl, which was stored at 4 °C.

10 μL of Ab_2 of AFP at 1.0 mg mL^{-1} was added into 400 μL of nanoAu/CNH suspension, followed by gently stirring at room temperature for 1 h. The resulting mixture was centrifuged at 3800 rpm for 10 min at 4 °C. The sediment was washed three times with pH 7.4 PBS to remove the unconjugated Ab_2 and dispersed in 400 μL of pH 7.4 PBS containing 1% BSA at 4 °C for 0.5 h to block the remaining exposed surface of nanogolds. Following a centrifugation at 3500 rpm for 10 min, the precipitate named as Ab_2/nanoAu/CNH was dispersed in 400 μL of 10 mM pH 7.4 PBS containing 0.1% BSA.

2.4 Preparation of Immunosensor

The immunosensor was constructed by covalently assembling Ab_1 on CS modified electrode (Scheme 1B). The screen printed carbon electrode (SPCE) system containing graphite working electrode (2 mm in diameter), graphite auxiliary electrode and Ag/AgCl reference electrode was firstly fabricated according to our previous report [26]. 1.5 μL of 0.25 mg mL^{-1} CS was then coated onto the working electrode and dried at room temperature. After activation with 2.5% GA (in 50 mM pH 7.4 PBS) for 2 h, 1.0 μL of 0.2 mg mL^{-1} Ab_1 of AFP was dropped onto the electrode and reacted at room temperature for 1h and then 4 °C overnight in a 100% moisture-saturated environment. Subsequently, excess Ab_1 were washed out with washing buffer. 20 μL of blocking buffer was finally dropped onto the SPCE and incubated for 1h at room temperature to block possible remaining active sites against nonspecific adsorption.

2.5 Immunoassay Procedure

A sandwich-type immunoassay was performed by incubating 5 μL of AFP standard solution or serum sample on the immunosensor and 5 μL of Ab_2/nanoAu/CNH for 30 min at 37 °C, respectively. Following a washing step, 50 μL of 0.1 M HCl was dropped on the SPCE to perform the electrochemical oxidation of nanogold at a constant potential of +1.30 V for 30 s, and immediately the DPV detection from +0.50 to +0.15 V, with a step potential of 4 mV, a pulse amplitude of 50 mV and a pulse period of 0.2 s, was performed to record the electrochemical signal produced on working electrode for AFP detection.

3 Results and Discussion

3.1 Characterization of Ab_2/nanoAu/CNH

TEM was used to characterize the formation of nanoAu/CNH. As shown in Figure 1A, after oxidation treatment the carboxylated SWCNHs maintained the dahlia-like nanostructure with a diameter of about 80–100 nm. Using positively charged PDDA as bridge, the $AuCl_4^-$ could be electrostatically absorbed on the surface of SWCNHs to produce nanogold by chemical reduction, which showed numerous uniformly distributed nanoparticles with a diameter of about 7 nm on the surface of SWCNHs (Figure 1B). The formation of nanoAu/CNH was further confirmed by XPS characterization (Figure 1C). Compared with the spectrum of bare carboxylated SWCNHs (curve a), only the spectrum of nanoAu/CNH showed obviously the Au4f peaks at 82.5 and 86.2 eV (curve b).

The nanoAu/CNH could be easily functionalized with Ab_2 via the inherent interaction between protein and nanogold to form the tracing tag [27]. As seen from Figure 1D, the XPS spectrum of Ab_2/nanoAu/CNH bioconjugate showed an obvious N1s peak at 398.8 eV (curve b), while no N1s peak was observed in the XPS spectrum of nanoAu/CNH (curve a). This result confirms the successful functionalization of nanoAu/CNH with Ab_2.

3.2 Characterization of the Immunosensor

The surface morphologies of the bare SPCE, CS modified SPCE and the immunosensor were characterized by SEM. As shown in Figure 2A, the surface of bare SPCE was inhomogeneous and uneven. After the coating of CS on SPCE, a uniform and smooth structure was observed due to the excellent film forming ability of CS (Figure 2B). Upon the covalent assembly of Ab_1 on CS modified SPCE by GA cross-linking, an obvious aggregation of the trapped biomolecules was observed (Figure 2C). This result indicated the immobilization of Ab_1 on the SPCE and the successful fabrication of the immunosensor.

3.3 Optimization of Detection Conditions

The ratio of Ab_2 to nanoAu/CNH was firstly optimized to be 1:10 (w/w). The other detection conditions were then optimized at this ratio. Figure 3A shows the effect of pre-oxidation potential on DPV response. With the increasing oxidation potential from +1.20 to +1.40 V, the DPV response increased and reached the maximum value at +1.30 V. At too high potential, the surface of SPCE would be destructed, which led to greatly decrease of the DPV response. Therefore, +1.30 V was selected as the

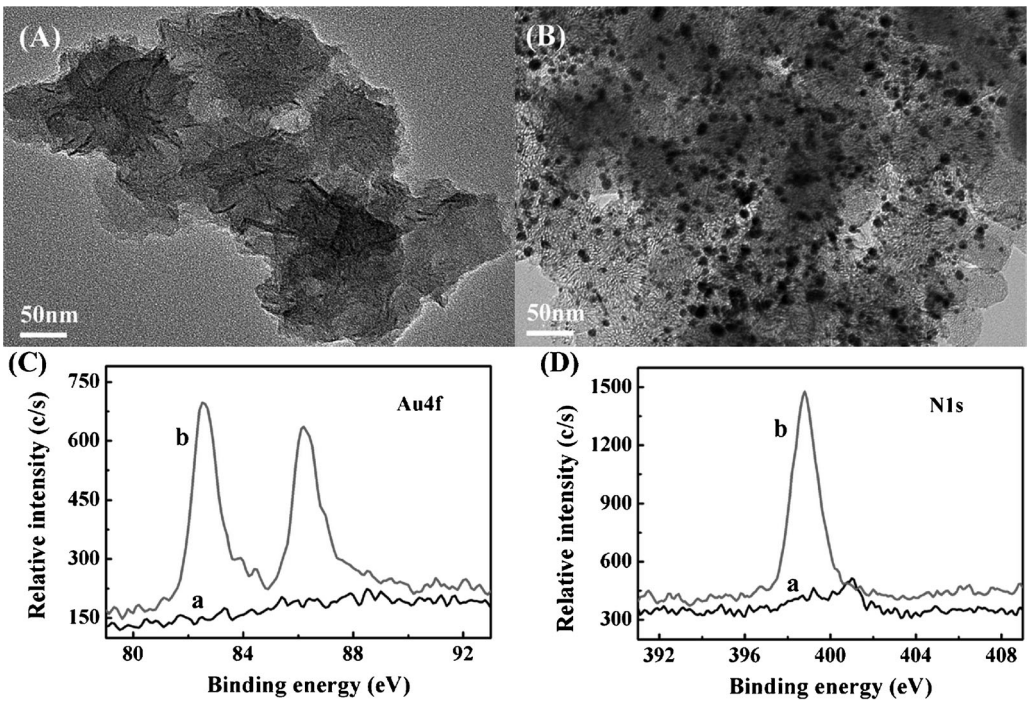

Fig. 1. TEM images of (A) carboxylated SWCNHs and (B) nanoAu/CNH, (C) XPS spectra of SWCNHs (a) and nanoAu/CNH (b), (D) XPS spectra of nanoAu/CNH (a) and Ab_2/nanoAu/CNH (b).

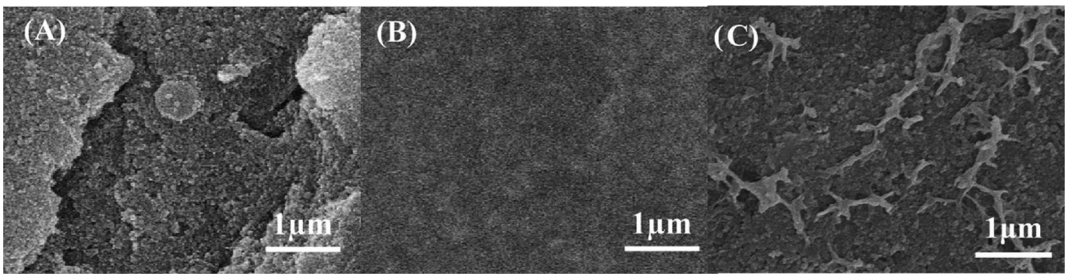

Fig. 2. SEM images of (A) bare SPCE, (B) CS modified SPCE, and (C) immunosensor.

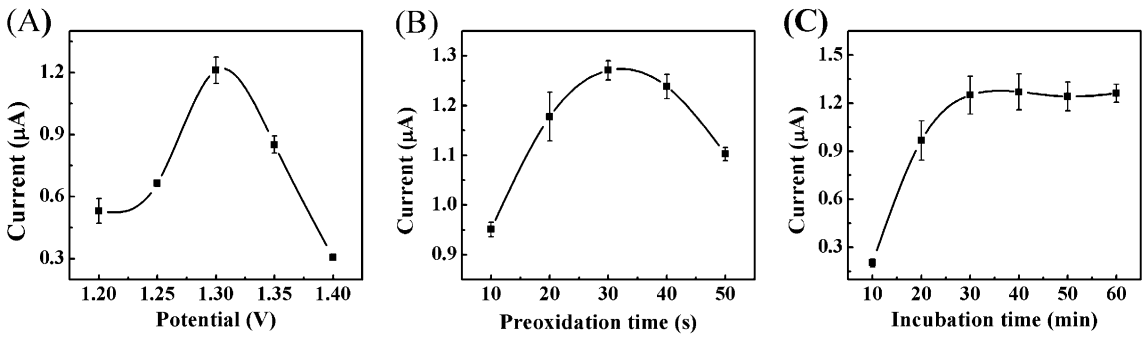

Fig. 3. Effects of (A) oxidation potential, (B) oxidation time, and (C) incubation time on DPV response to 1 ng mL^{-1} AFP at the immunosensor.

optimal oxidation potential, at which the DPV response increased with the increasing oxidation time and reached the maximum value at the time of 30 s (Figure 3B). Beyond 30 s, the peak current decreased greatly due to the diffusion of the formed $AuCl_4^-$ away from electrode surface. Consequently, 30 s was chosen as the optimal oxidation time.

The incubation time is an important parameter affecting the analytical performance of immunoassay. At room temperature, the DPV response increased with increasing

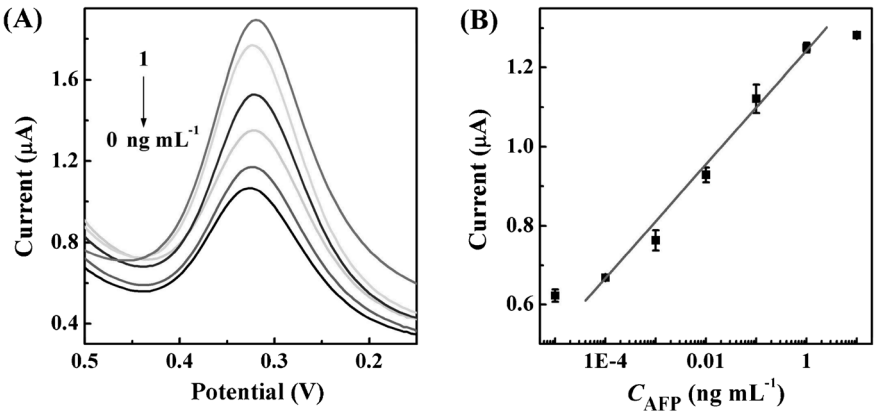

Fig. 4. (A) DPV responses and (B) calibration curve for the detection of AFP.

incubation time and trended to a constant value after an incubation time of 30 min (Figure 3C). Longer incubation time did not improve the response, indicating that 30 min was sufficient for saturated binding between the analyte and the antibody. Thus, an incubation time of 30 min was selected for the sandwich-type immunoassay.

3.4 Analytical Performance

With the sandwich immunoreaction, the nanoAu/CNH was assembled on the immunosensor surface to produce electrochemical signal for the detection of analyte. Under optimum conditions, the DPV response increased proportionally with the increasing concentrations of AFP (Figure 4A). The calibration plot showed a good linear relationship between the DPV peak current and the logarithm value of the AFP concentration in the range of 0.1 pg mL^{-1} to 1.0 ng mL^{-1} with a correlation coefficient of 0.9985 (Figure 4B). The detection limit corresponding to a signal-to-noise ratio of 3 was 0.07 pg mL^{-1}, which was much lower than those reported previously [28–31]. The sensitivity as the slope of the calibration curve was 144.11 nA mL ng^{-1}, which was much larger than that reported previously in immunoassay using HRP labeled secondary antibody [13], and even approaching that in immunoassay with gold nanoparticle congregate based amplification [15]. The good analytical performance of the proposed immunoassay method, including ultralow detection limit and wide linear range over 4 orders of magnitude for protein biomarker, benefited from the combination of the new nanoAu/CNH label which was featured with high loading of nanogold on CNH and the ultrasensitive electrochemical stripping analysis of metal nanoparticles.

In addition, the nonspecific binding character of the proposed immunoassay was evaluated with a CEA immunosensor prepared with the same preparation procedure. The DPV response on the CEA immunosensor incubated with 0.5 ng mL^{-1} AFP was 0.737 ± 0.041 μA, which was similar to the noise of 0.674 ± 0.087 μA on immunosensor, indicating few nonspecific binding occurred between antigen and nonspecific recognition elements.

Table 1. Assay results of AFP in clinical serum samples using the proposed and reference methods.

Sample no	1	2	3	4
Proposed method (pg mL^{-1}) [a]	36.1 ± 1.3	22.7 ± 0.2	30.8 ± 0.8	43.7 ± 1.1
Reference method (ng mL^{-1})	3.41	2.21	3.20	4.32
Relative error (%)	5.87	2.71	−3.75	1.16

[a] The serum samples were diluted at 100 times prior to assay using the proposed method.

3.5 Reproducibility and Precision of Immunosensor

Both the intra-assay and inter-assay precisions of the immunosensor were examined by parallel immunoassay for 5 times with 100 pg mL^{-1} AFP. The relative standard deviations (*RSD*) were 4.6% and 5.7%, respectively, showing good precision and acceptable fabrication reproducibility. In addition, after the immunosensor was stored dry at 4 °C with a period of 1 week, 93% of the initial response was remained, indicating an acceptable stability of the immunosensor.

3.6 Application in Detection of Serum Sample

To evaluate the reliability and application potential of the proposed immunoassay, the assay results of AFP in clinical serum samples obtained by the designed immunosensors ($n = 3$) were compared with the reference values from the commercial electrochemiluminescent testing. Due to the high detection sensitivity of the proposed method, serum samples were diluted 100 times with 10 mM pH 7.4 PBS prior to assay. The results were listed in Table 1. An acceptable agreement with relative errors less than 5.87% indicated good accuracy of the proposed method for the detection of clinical samples.

4 Conclusions

A nanoAu/CNH structure was designed as a label to combine with a disposable immunosensor for highly efficient electrochemical immunoassay of tumor marker. The nanoAu/CNH label could be synthesized conveniently by one-pot in situ growth of nanogold on carboxylated SWCNH and be easily functionalized with signal antibody. The high loading of nanogold on CNH greatly amplified the detection signal and hence improved the detection sensitivity. With the electrochemical stripping analysis of the nanogold, the proposed immunoassay method showed a wide detection range and an ultralow detection limit for AFP. The detection step excluded the deoxygenation procedure, leading to a simplification of the immunoassay. The proposed method and the nanoAu/CNH label exhibited good analytical performance for protein biomarker with easy design, simple operation, low cost, high sensitivity and acceptable accuracy, showing great promise in clinical application.

Acknowledgements

This work was financially supported by the National Basic Research Program (2010CB732400), the *National Natural Science Foundation of China* (21075055, 21135002, 21121091 and 21105046), PhD Fund for Young Teachers (20110091120012), the Leading Medical Talents Program from the *Department of Health of Jiangsu Province*, and the *Natural Science Foundation of Jiangsu* (BK2011552).

References

[1] S. P. Song, Y. Qin, Y. He, Q. Huang, C. H. Fan, H. Y. Chen, *Chem. Soc. Rev.* **2010**, *39*, 4234.
[2] J. Wu, Z. F. Fu, F. Yan, H. X. Ju, *Trac–Trends Anal. Chem.* **2007**, *26*, 679.
[3] Q. F. Li, D. P. Tang, J. Tang, B. L. Su, J. X. Huang, G. N. Chen, *Talanta* **2011**, *84*, 538.
[4] H. F. Chen, D. P. Tang, B. Zhang, B. Q. Liu, Y. L. Cui, G. N. Chen, *Talanta* **2012**, *91*, 95.
[5] Y. Zhuo, W. J. Yi, W. B. Lian, R. Yuan, Y. Q. Chai, A. Chen, C. M. Hu, *Biosens. Bioelectron.* **2011**, *26,* 2188.
[6] A. Ambrosi, M. T. Castaneda, A. J. Killard, M. R. Smyth, S. Alegret, A. Merkoci, *Anal. Chem.* **2007**, *79*, 5232.
[7] R. J. Cui, H. P. Huang, Z. Z. Yin, D. Gao, J. J. Zhu, *Biosens. Bioelectron.* **2008**, *23*, 1666.
[8] J. Tang, B. L. Su, D. P. Tang, G. N Chen, *Biosens. Bioelectron.* **2010**, *25*, 2657.
[9] X. Yu, B. Munge, V. Patel, G. Jensen, A. Bhirde, J. D. Gong, S. N. Kim, J. Gillespie, J. S. Gutkind, F. Papadimitrakopoulos, J. F. Rusling, *J. Am. Chem. Soc.* **2006**, *128*, 11199.
[10] R. Malhotra, V. Patel, J. P. Vaqué, J. S. Gutkind, J. F. Rusling, *Anal. Chem.* **2010**, *82*, 3118.
[11] D. Du, Z. X. Zou, Y. Shin, J. Wang, H. Wu, M. H. Engelhard, J. Liu, I. A. Aksay, Y. H. Lin, *Anal. Chem.* **2010**, *82*, 2989.
[12] Y. F. Wu, C. L. Chen, S. Q. Liu, *Anal. Chem.* **2009**, *81*, 1600.
[13] V. Mani, B. V. Chikkaveeraiah, V. Patel, J. S. Gutkind, J. F. Rusling, *ACS Nano* **2009**, *3*, 585.
[14] M. Dequaire, C. Degrand, B. Limoges, *Anal. Chem.* **2000**, *72*, 5521.
[15] J. A. Ho, H. C. Chang, N. Y. Shih, L. C. Wu, Y. F. Chang, C. C. Chen, C. Chou, *Anal. Chem.* **2010**, *82*, 5944.
[16] S. Pinijsuwan, P. Rijiravanich, M. Somasundrum, W. Surareungchai, *Anal. Chem.* **2008**, *80*, 6779.
[17] B. P. Ting, J. Zhang, M. Khan, Y. Y. Yang, J. Y. Ying, *Chem. Commun.* **2009**, *41*, 6231.
[18] G. S. Lai, J. Wu, H. X. Ju, F. Yan, *Adv. Funct. Mater.* **2011**, *21*, 2938.
[19] G. D. Liu, J. Wang, J. Kim, M. R. Jan, *Anal. Chem.* **2004**, *76*, 7126.
[20] L. Y. Chen, C. L. Chen, R. N. Li, Y. Li, S. Q. Liu, *Chem. Commun.* **2009**, *19*, 2670.
[21] Q. N. Xu, F. Yang, J. P. Lei, C. Leng, H. X. Ju, *Chem. Eur. J.* **2012**, *18*, 4994.
[22] R. Yuge, T. Ichihashi, Y. Shimakawa, Y. Kubo, M. Yudasaka, S. Iijima, *Adv. Mater.* **2004**, *16*, 1420.
[23] M. F. Zhang, T. Yamaguchi, S. Iijima, M. Yudasaka, *J. Phys. Chem. C.* **2009**, *113*, 11184.
[24] C. Yang, H. Noguchi, K. Murada, M. Yudasaka, A. Hashimoto, S. Iijima, K. Kaneko, *Adv. Mater.* **2005**, *17*, 866.
[25] K. M. Urita, S. Seki, S. Utsumi, D. Noguchi, H. Kanoh, H. Tanaka, Y. Hattori, Y. Ochiai, N. Aoki, M. Yudasaka, S. Iijima, K. Kaneko, *Nano Lett.* **2006**, *6*, 1325.
[26] J. Wu, J. H. Tang, Z. Dai, F. Yan, H. X. Ju, N. E. Murrc, *Biosens. Bioelectron.* **2006**, *22*, 102.
[27] C. Sönnichsen, B. M. Reinhard, J. Liphardt, A. P. Alivisatos, *Nat. Biotechnol.* **2005**, *23*, 741.
[28] Y. X. Dai, Y. Y Cai, Y. F. Zhao, D. Wu, B. Liu, R. Li, M. H. Yang, Q. Wei, B. Du, H. Li, *Biosens. Bioelectron.* **2011**, *28*, 112.
[29] J. Tang, D. P. Tang, B. L. Su, Q. F. Li, B. Qiu, G. N. Chen, *Electrochim. Acta* **2011**, *56*, 8168.
[30] B. L. Su, D. P. Tang, J. Tang, Q. F. Li, G. N. Chen, *Anal. Biochem.* **2011**, *417*, 89.
[31] H. L. Su, R. Yuan, Y. Q. Chai, Y. Zhuo, *Biosens. Bioelectron.* **2012**, *33*, 288.

